



Enhanced photocatalytic activity of ZnO nanostructures deposited on mesh through electrochemical deposition and thermal oxidation

Chantana AIEMPANAKIT¹, Thongchai PHANTAPORN², and Kamon AIEMPANAKIT^{2,*}

¹ Division of Physics, Faculty of Science and Technology, Rajamangala University of Technology Thanyaburi, Pathumthani, 12110, Thailand

² Department of Physics, Faculty of Science and Technology, Thammasat University, Pathumthani, 12121, Thailand

*Corresponding author e-mail: kamon.aie@hotmail.com

Received date:

1 March 2022

Revised date

3 May 2022

Accepted date:

8 May 2022

Keywords:

ZnO nanostructure;
Thermal oxidation;
Photocatalytic activity

Abstract

This article reported that the properties of zinc oxide (ZnO) nanostructures were modified by the thermal oxidation process at different temperatures in the range of 200°C to 600°C for 1 h. The Zn films were deposited on a stainless steel mesh by using the electrochemical deposition technique. The elemental composition of Zn and O was exhibited via energy-dispersed X-ray spectroscopy in which the atomic ratio of O/Zn increased with the increase of oxidation temperature. The results showed that oxidation temperature has a significant effect on the morphological and crystal structure. The nanosheet structure of the as-deposited film transferred to the intermixing of porous nanosheet and urchin-like structure at the oxidation temperature of 600°C while the crystallinities of mixing Zn and ZnO were improved to only ZnO when increasing the oxidation temperature. ZnO films were tested for photocatalytic activity in methylene blue under various ultraviolet irradiation times. The best condition of ZnO for photocatalytic activity was an oxidation temperature of 600°C with the highest crystallinity and surface area that showed the highest decomposition rate and percentage degradation of $8.150 \times 10^{-3} \text{ min}^{-1}$ and 74.06%, respectively.

1. Introduction

ZnO is a direct bandgap semiconductor with an energy band gap of 3.3 eV at room temperature, and generally, the structures of ZnO are hexagonal wurtzite, cubic zinc band, and cubic rock salt [1-3]. Hexagonal is the most common structure, characterized by a variety of nanostructures such as nanowires, nanorods, and nanosheets [4]. Nanostructured ZnO can absorb light or emit light in short wavelengths and has a highly effective surface area. Therefore, ZnO is preferable for the creation of laser diode devices, gas sensors, optoelectronic devices, solar cell devices, and photocatalytic reactions [5-7]. ZnO films were synthesized by various techniques to develop the nanostructure such as thermal evaporation [8], hydrothermal techniques [9], RF magnetron sputtering [10], physical vapor deposition processes [11], and chemical vapor deposition [12]. These techniques have complex procedures and equipment preparation, as well as long processing times. In recent years, ZnO films with high purity and quality were synthesized by thermal oxidation (TO) as a simple and cost-effective method for the synthesis of ZnO nanostructures [13,14]. This technique was employed in the development of film structures including crystallinity and morphology.

The photocatalytic attributes of thin film are very attractive due to their properties depending on morphology, crystal size, and modified nanostructures. Besides titanium dioxide, ZnO can be considered as a highly studied and modified structure [15]. Dikici [16] reported that TO affected ZnO nanostructures deposited via electrodeposition from

Zn films and affected their photocatalytic activities. The best photocatalytic of ZnO nanostructures was exhibited at an oxidation temperature of 800°C. Fan Wu *et al* [17] studied the synthesis of metal oxide nanosheets by the TO process on a stainless steel mesh (SSM). Increasing the temperature from 1000°C to 1100°C affected the nanostructures leading to a change from 2D to 3D when the oxidation time was more than 1 h. Moreover, Rojas-Chavez *et al* [18] studied the formation of ZnO structures on zinc foils in different chemical conditions with the TO process. The ZnO nanowire structure was synthesized at 400°C for 2 h. This can be used in optoelectronic devices. Among these studies, the effects of the nanostructure of ZnO films modified by TO on photocatalytic activity are rarely examined. The relationship of TO with the elemental composition of ZnO film with a modified structure is also mentioned in few studies.

In this work, nanostructured ZnO films were synthesized on SSM. Electrochemical deposition and TO were used to provide the ZnO nanostructure. There is a simple process that can prepare the film efficiently and quickly. The influences of oxidation temperature on the structural and photocatalytic properties of ZnO films were studied. We discuss the relationship of morphology, structure, and elemental composition of the ZnO films as well as photocatalytic properties under various UV irradiation times.

2. Experimental details

2.1 Preparation of ZnO films

Zn films were prepared on SSM via electrochemical deposition. A $3 \times 2 \text{ cm}^2$ SSM substrate was cleaned with an ultrasonic cleaner using deionized water, acetone, and 2-propanol for 15 min, respectively. The electrochemical method was used to prepare Zn with the solution of zinc sulfate ($\text{ZnSO}_4 \cdot 7\text{H}_2\text{O}$) at a concentration of 0.50 M and a volume of 50 mL. The SSM and the zinc plate were used as the cathode (-) and the anode (+), respectively. All electrodes were dipped in the $\text{ZnSO}_4 \cdot 7\text{H}_2\text{O}$ solution and adjusted to the applied voltage of 4.0 V for 5 min. All samples were cleaned with deionized water and dried in the air. The as-deposited Zn films were thermally oxidized at various oxidation temperatures from 200°C to 600°C for 1 h in the ambient air.

2.2 Characterization

The crystal structures of all ZnO films were determined by using the X-ray diffractometer (XRD, Bruker D2 Phaser) with Cu-K α radiation at a wavelength of 1.5406 Å (applied voltage of 30 kV, and applied current of 10 mA) which recorded at 2θ from 20° to 80° with a step size of 2°/min. The field emission scanning electron microscope (FE-SEM, JEOL 6060) with energy dispersed X-ray spectroscopy (EDX) was carried out to study the surface morphology and elemental composition of the ZnO film. The methylene blue (MB) solution was used to perform experiments at a concentration of 0.05 mM with volume of 10 mL before irradiation with two UV lamps (SANTORY, Backlight lamp, F10T8BL 10 W) at wavelength of 365 nm and intensity of 0.35 $\text{mW} \cdot \text{cm}^{-2}$ for testing the photocatalytic activity of ZnO film. This MB solution determined the relationship between the absorption of the solution and its concentration according to Lambert's rules. The distance between the UV light source and MB solution was 100 mm. Absorption of MB is measured using a spectrophotometer (GENESYS 10S, Thermo Scientific). The UV irradiation was used to determine the photocatalytic activity of ZnO film at a time period in the range of 0 min to 120 min.

3. Results and discussion

3.1 Structural and morphological properties

Figure 1 shows the XRD patterns of SSM and all conditions of the ZnO films. The results showed that the XRD peaks of SSM indicated iron-nickel structures (PDF 01-071-5097) at the (111), (110), (200), and (220) planes which corresponded with 2θ of 43.8°, 44.7°, 51.1°, and 74.9°, respectively. As-deposited Zn showed the XRD peaks of Zn at (100), (101), and (102) planes (PDF 00-011-1244) and the only XRD peak of ZnO at (101) plane (PDF 01-082-3143) which was the highest intensity of a standard peak. The XRD peaks of Zn transferred to ZnO films when increasing the oxidation temperature above 200°C. At an oxidation temperature of 600°C, the XRD peaks were found with crystal plane orientations of (100), (002), (101), (102), (110), (103), (200), and (201) which correspond to 2θ of 31.9°, 34.6°, 36.4°, 47.8°, 56.9°, 63.2°, 66.7°, and 69.5°, respectively. It indicated that ZnO films were of a hexagonal wurtzite structure. Increasing the oxidation temperature improved the crystallinity of ZnO for which the average crystallite sizes of ZnO films were 17.69 nm and

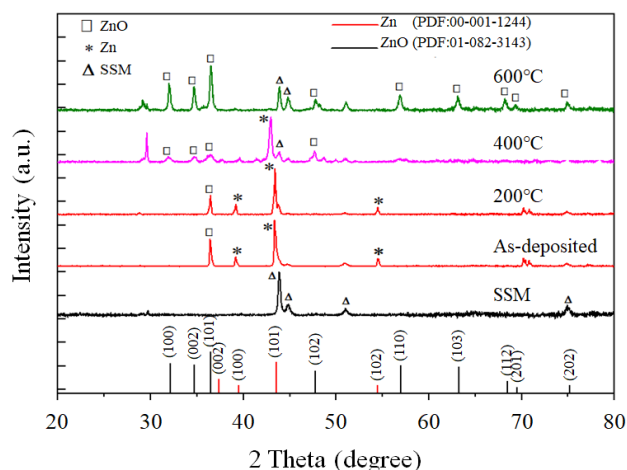


Figure 1. XRD of SSM, as-deposited, and thermally oxidized ZnO films at oxidation temperatures of 200°C, 400°C, and 600°C.

29.04 nm at oxidation temperatures of 400°C and 600°C, respectively, which were calculated using the equation of Scherrer [19]. Therefore, an oxidation temperature of 400°C and above for 1 h was sufficient to promote the crystal structure of ZnO films. XRD peak at about 29.6° (unlabeled) for oxidation temperature of 400°C and 600°C may be the peak of stainless steel oxidized such as Fe_3O_4 .

Figure 2 shows the morphology from the FE-SEM images of SSM and all conditions of ZnO films deposited on SSM. We found that SSM in Figure 2(a) showed a smooth surface while as-deposited films in Figure 2(b) exhibited high roughness and large grain with dense film and insertion of the nanosheet structure through the surface. The as-deposited showed the structure of a 2 dimensional nanosheet on micro-grain due to the reaction of $\text{ZnO}_4 \cdot 7\text{H}_2\text{O}$ during the electrochemical process [16,17]. Moreover, the amounts of nanosheet of ZnO were enhanced with the oxidation temperature at 200°C as shown in Figure 2(c) while an oxidation temperature of 400°C in Figure 2(d) affected a change from a dense nanosheet to a porous nanosheet structure. At an oxidation temperature of 600°C, the ZnO morphology presented an urchin-like structure mixed with the nanosheet structure that was porous throughout the surface (see Figure 2(e)). The morphology transformation of as-deposited Zn films by TO at oxidation temperature of 400°C and above is related to the melting point of Zn which was 419.5°C [20]. These can also be explained that the growth mechanism of the ZnO nanostructures is controlled by vapor-solid (VS) mechanism more than vapor-liquid-solid (VLS) mechanism because of a catalyst-free synthesis of ZnO [21-23] which is called self-catalysis. These results showed that the ZnO nanostructure enhanced the active surface area with highly porous nanosheet and urchin-like structures.

The elemental composition of ZnO nanosheet and urchin-like was obtained by EDX analysis as shown in Figure 3. The elemental composition of the SSM exhibited dominance of Fe, Cr, C, Ni O, and Si at 56.62, 16.22, 15.28, 6.44, 3.87, and 1.66 at%, respectively. The as-deposited and thermally oxidized ZnO films showed changes in both Zn and O elements. Figure 4 shows the relationship of atomic ratios in which Zn decreased from 80.52 at% to 37.88 at% and O increased from 19.48 at% to 50.88 at% with increasing oxidation temperature. Meanwhile, increased O content corresponded to the ZnO nanostructures changing from dense to porous nanosheet and

urchin-like structure with increasing oxidation. The result exhibited the stoichiometric control of ZnO by adjusting the oxidation temperature. At an oxidation temperature of 600°C, O content was found to be

approximately 50 at% which corresponded with the report of Jouya *et al.* [8].

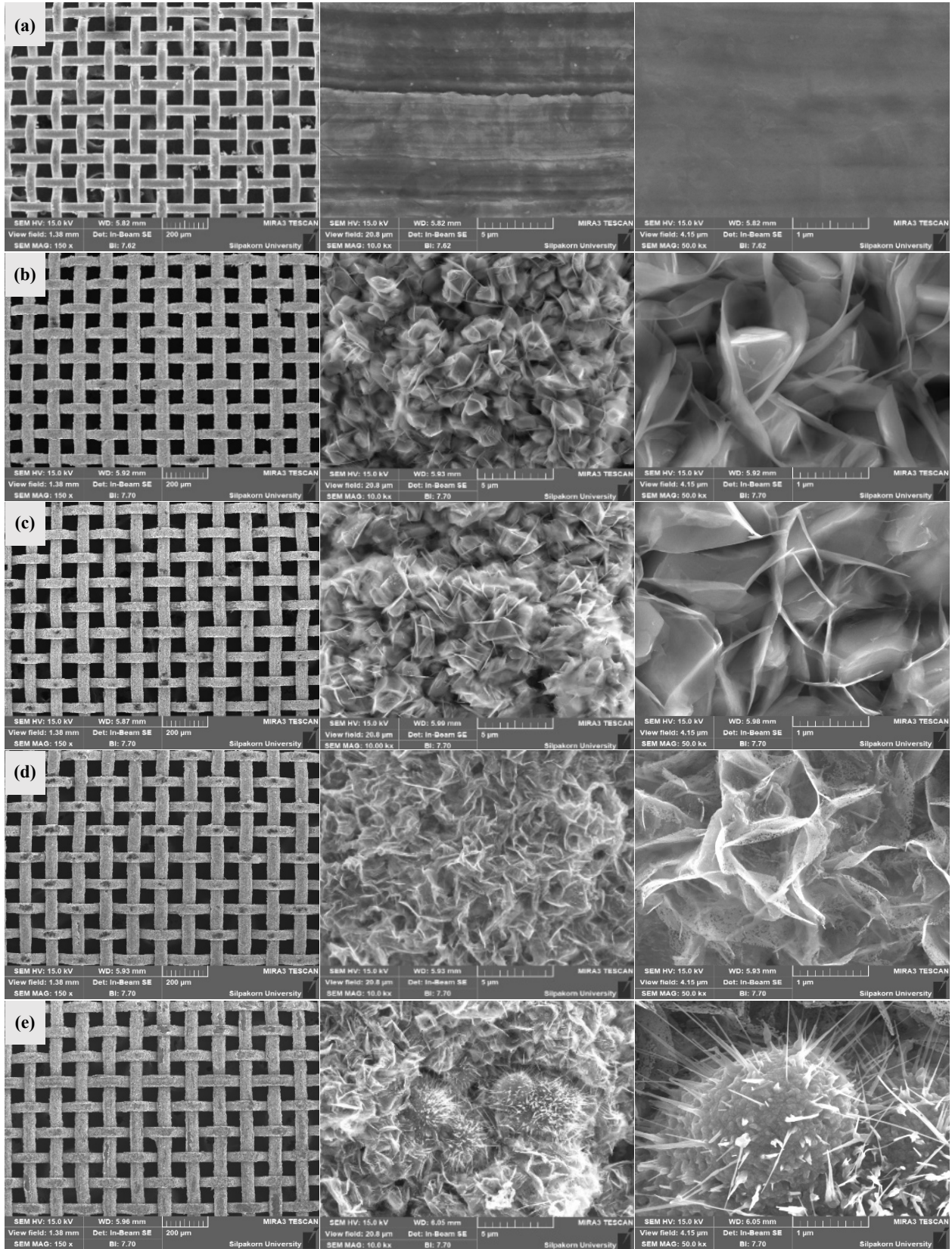


Figure 2. FE-SEM images of (a) SSM, (b) as-deposited, and thermally-oxidized ZnO at oxidation temperatures of (c) 200°C, (d) 400°C, and (e) 600°C.

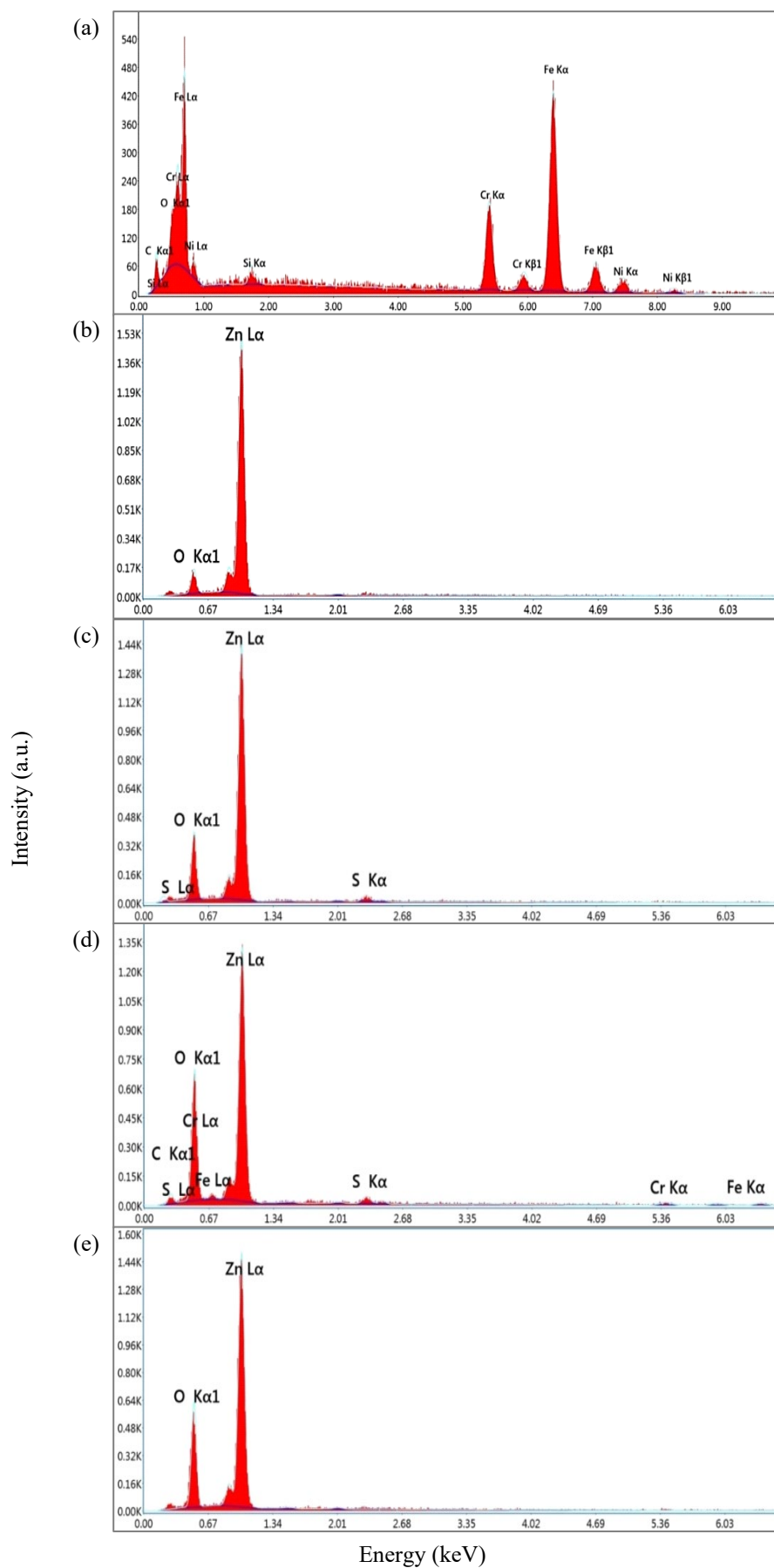


Figure 3. EDS analysis of (a) SSM, (b) as-deposited, and thermally-oxidized ZnO films at oxidation temperatures of (c) 200°C, (d) 400°C, and (e) 600°C.

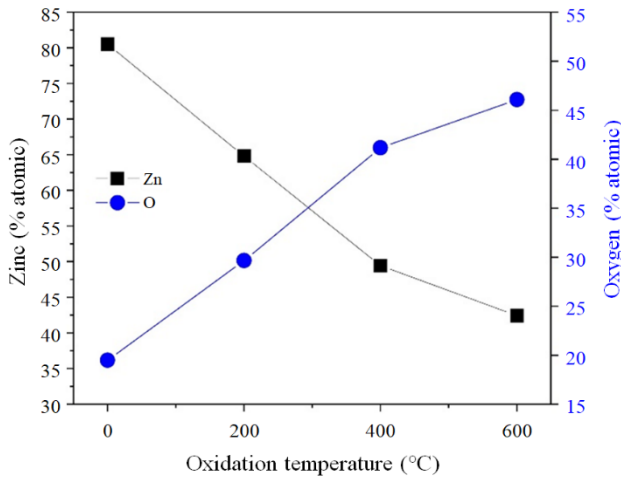


Figure 4. Relationships between atomic percentages of Zn and O in ZnO films at different oxidation temperatures.

3.2 Photocatalytic activity

The relationship between the absorbance value at a wavelength of 664 nm and the concentration of the MB from 0.01 to 0.05 mM was obtained with a linear curve. According to Lambert-Beer's law [24], the linear relationship between the absorbance values (y) and the concentration of the MB (x) can be calculated from the equation of $y = 0.03411x$ with regression (R^2) of 0.99019. Figure 5 shows the photodecolorizations of MB (C/C_0), where C_0 represents the initial concentration of MB and C is the concentration of MB in the dark (without UV) and after UV irradiation for samples UV (without films), as-deposited, at 200°C, 400°C, and 600°C. Slow degradation of MB was found in the dark with C/C_0 of 0.90 at a time of 120 min. The decrease of photodecolorization of MB in the dark was just caused by adsorption of MB upon surface contact with the container. Under UV irradiation at samples of UV, as-deposited, 200°C, 400°C, and 600°C showed C/C_0 of 0.70, 0.58, 0.47, 0.38, and 0.29, respectively, at an irradiation time of 120 min. Oxidation temperature was found to play an important role in the photodecolorizations of MB. At an oxidation temperature of 600°C, the urchin-like structure was promoted with greater crystallinity of sufficient oxygen in ZnO films. These caused the enhancement of effective surface area which increased the efficiency of light absorption [25-28]. Photocatalytic activity occurs when enough light energy is obtained as photon energy ($h\nu$) for the reaction to occur; this energy is called activation energy. When the catalyst is stimulated by light, the electrons from the valence band move to the conduction band, creating electron (e^-) and hole (h^+) pairs, which are scattered on the surface of the ZnO films (A1). Positive holes react with hydroxide ions (OH^-) or water (H_2O) to form a hydroxyl radical (OH^\bullet) as presented in (A2) and (A3), which is the oxidant in the photocatalytic process. The adsorbed oxygen (O_2) on the surface of the film occurred in the reduction reaction which is an electron receptor to form the superoxide ions or superoxide radicals ($O_2^{\bullet-}$) as shown in (A4). These radicals can degrade MB.

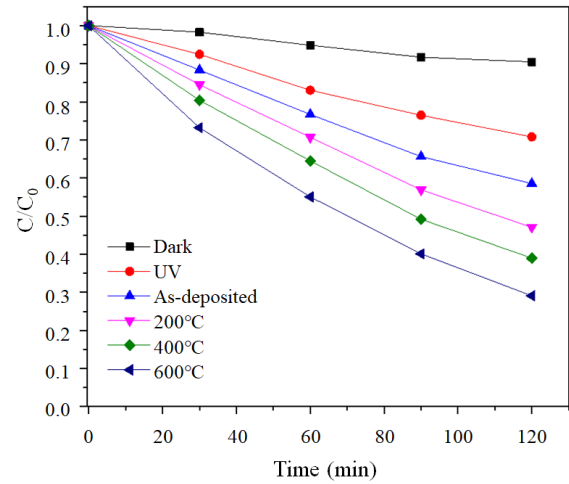
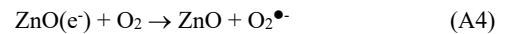
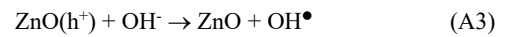
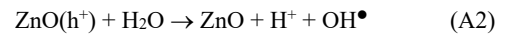
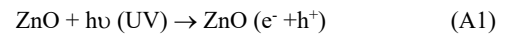


Figure 5. Photodecolorizations of MB under UV irradiation with and without ZnO films and MB in the dark.



In the mechanism of the photodecolorization of MB, in the presence of catalysts, the excited state of MB^* with photon energy injects an electron into the conduction band (B1). The MB is then converted to a cationic radical that undergoes degradation to yield products according to (B2) to (B4). The hydroxyl radical and superoxide radicals existing on the surface of ZnO accelerated the degradation of MB ((B3)-(B4)).

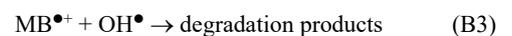
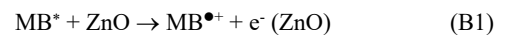


Figure 6 shows the changing of $\ln(C_0/C)$ with respect to time under UV irradiation. The relationship of $\ln(C_0/C)$ with the irradiation period showed linearity and increased inclination with increasing oxidation temperatures of 200°C, 400°C, and 600°C. From the equation of $\ln(C_0/C) = kt$, the decomposition rate constant (k) of all samples is optical decolorization kinetics. The equation used in the calculation follows the model of Langmuir-Hinshelwood [29]. Most recently, M. Ballesteros-Balbuena *et al* [28] reported that the ZnO nanostructures of urchin-like and needle-like forms were grown by TO at temperatures of 500°C to 600°C in the air for 2 h from

the zinc plate. This condition showed the best decomposition rate of $4.398 \times 10^{-3} \text{ min}^{-1}$ with a concentration of MB solution of $10 \text{ mg}\cdot\text{L}^{-1}$ and two UV lamps (20 W) irradiated at a wavelength of 365 nm for 3 h. In this study, the exhibited decomposition rates for UV, in the dark, as-deposited, at oxidation temperatures of 200°C, 400°C, and 600°C were 0.600×10^{-3} , 2.300×10^{-3} , 3.500×10^{-3} , 4.780×10^{-3} , 6.060×10^{-3} , and $8.150 \times 10^{-3} \text{ min}^{-1}$, respectively. The sample at an oxidation temperature of 600°C determined that the decomposition rate of the MB solution was 1.85 times faster than in previous work [29].

Figure 7 shows the percentage degradation of MB for all conditions calculated by the equation of $(C_0 - C_t) \times 100 / C_0$ where C_t is the concentration of MB at UV irradiation times of 120 min. The conditions of in the dark, UV, as-deposited, and thermally-oxidized ZnO nanostructures at oxidation temperatures of 200°C, 400°C, and 600°C were evaluated at 3.50%, 49.19%, 54.45%, 57.48%, 65.25%, and 74.06%, respectively. The percentage degradation for the intermixing porous nanosheet and urchin-like structure of ZnO was higher than for other conditions. Moreover, when considering conditions of UV without ZnO film, and thermally oxidized ZnO at an oxidation temperature of 600°C, there was a difference in percentage degradation of 24.87% and a difference in decomposition rate of $5.850 \times 10^{-3} \text{ min}^{-1}$.

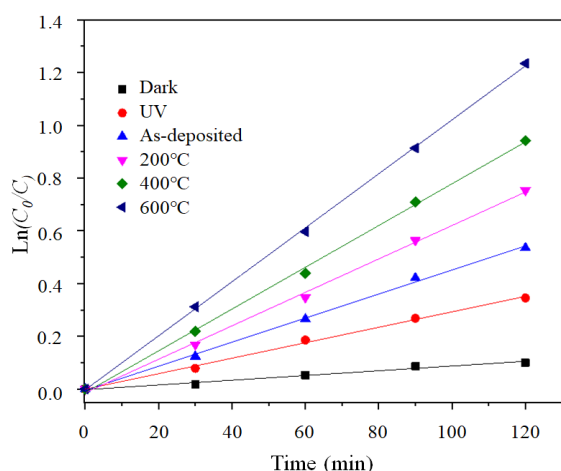


Figure 6. Plots of the first order reaction of MB in the dark and MB under UV irradiation with and without ZnO films.

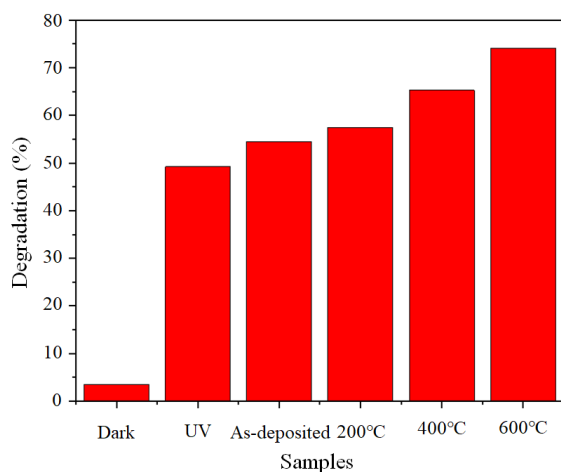


Figure 7 Percentage degradation of MB of in the dark and under UV irradiation with and without ZnO films.

The significant effect of MB degradation is associated with high crystallinity which obtained sufficient oxygen at 50.88 at% as shown in Figure 1 and the surface morphology consistent with FE-SEM images can be seen in Figure 2(e). This occurs because the photocatalytic activity with ZnO films is influenced by their crystal structure, porosity, and specific surface area.

4. Conclusions

The nanostructured ZnO films were prepared successfully with the electrochemical deposition method on SSM and thermal oxidation at temperatures of 200°C, 400°C, and 600°C. Increased oxidation temperature affected the morphological nanostructure of the ZnO films leading to a change from dense nanosheet to intermixing porous nanosheet and urchin-like structure. The oxygen content and crystallinity of ZnO films were improved via increasing oxidation temperature. Enhanced photodecolorizations of MB suggested that the ZnO nanostructures showed developed morphological structure with a higher active surface area and crystallinity due to increased oxidation temperature. The obtained intermixing of porous nanosheet and urchin-like structure of ZnO film with an oxygen content of 50.88 at% at an oxidation temperature of 600°C has great practical potential with the highest decomposition rates of $8.150 \times 10^{-3} \text{ min}^{-1}$ and percentage degradation of 74.06%.

Acknowledgements

The authors gratefully acknowledge the financial support (SciGR31/2563) by the Faculty of Science and Technology, Thammasat University, Thailand. The authors would like to thank Department of Physics for providing the experimental facilities.

References

- [1] M. A. Borysiewicz, "ZnO as a functional material," *Crystals*, vol. 9, no. 10, 505 pp. 1-29, 2019.
- [2] K. Rajesh, O. Al-Dossary, K. Girish, and U. Ahmad, "Zinc oxide nanostructures for NO₂ gas-sensor applications: A Review," *Nano-Micro Letters*, vol. 7, no. 2, pp. 97-120, 2015.
- [3] C. B. Ong, L.Y. Ng, and A.W. Mohammad, "A review of ZnO nanoparticles as solar photocatalysts: synthesis, mechanisms and applications," *Renewable and Sustainable Energy Reviews*, vol. 81, pp. 536-551, 2018.
- [4] P. A. Hu, Y. Q. Liu, L. Fu, X. B. Wang, and D.B. Zhu, "Controllable morphologies of ZnO nanocrystals: nanowire attracted nanosheets, nanocartridges and hexagonal nanotowers," *Applied Physics A*, vol. 80, no. 1, pp. 35-38, 2005.
- [5] U. Ozgur, Ya. I. Alivov, C. Liu, A. Teke, M. A. Reshchikov, S. Dogan, V. Avrutin, S.-J. Cho, and H. Morkoç, "A comprehensive review of ZnO materials and devices," *Journal of applied physics*, vol. 98, p. 041301, 2005.
- [6] L. Yan, J. Li, W. Li, F. Zha, H. Feng, and D. Hu, "A photo-induced ZnO coated mesh for on-demand oil/water separation based on switchable wettability," *Materials Letters*, vol. 163, pp. 247-249, 2016.

- [7] M.-H. Hsu, and C.-J. Chang, "Ag-doped ZnO nanorods coated metal wire meshes as hierarchical photocatalysts with high visible-light driven photoactivity and photostability," *Journal of Hazardous Materials*, vol. 278, pp. 444-453, 2014.
- [8] M. Jouya, F. Taromian, and M. Afshari Abolkarlou, "Growth of Zn thin films based on electric field by thermal evaporation method and effect of oxidation time on physical properties of ZnO nanorods," *Journal of Materials Science: Materials in Electronics*, vol. 31, pp. 8680-8689, 2020.
- [9] P. Basnet, and S. Chatterjee, "Structure-directing property and growth mechanism induced by capping agents in nanostructured ZnO during hydrothermal synthesis - A systematic review," *Nano-Structures & Nano-Objects*, vol. 22, p. 100426, 2020.
- [10] B. Du, J. Jiang, J. Li, and W. ZHU, "Effects of ZnO magnetron sputtering on surface charge and flashover voltage of oil-impregnated paper," *High Voltage*, vol. 4, no. 4, pp. 308-315, 2019.
- [11] I. Haq, J. Jacob, K. Mehboob, K. Mahmood, A. Ali, N. Amin, and F. Ashraf, "Effect of annealing temperature on the thermoelectric properties of ZnO thin films grown by physical vapor deposition," *Physica B: Condensed Matter*, vol. 606, p. 412569, 2021.
- [12] J. Li, J. Cai, Z. Wu, J. Wang, and Y. Pei, "Numerical simulation and study of the metal-organic chemical vapor deposition growth of ZnO film," *Physics of Fluids*, vol. 31, p. 027104, 2019.
- [13] I. Mihailova, V. Gerbreder, E. Tamaniš, E. Sledevskis, R. Viter, and P. Sarajevs, "Synthesis of ZnO nanoneedles by thermal oxidation of Zn thin films," *Journal of Non-Crystalline Solids*, vol. 377, pp. 212-216, 2013.
- [14] D. Yuvaraj, and K.N. Rao, "Selective growth of ZnO nanoneedles by thermal oxidation of Zn microstructures," *Materials Science and Engineering: B*, vol. 164, pp. 195-199, 2009.
- [15] J. R. Torres-Hernández, E. Ramírez-Morales, L. Rojas-Blanco, J. Pantoja-Enriquez, G. Oskam, F. Paraguay-Delgado, and G. Pérez-Hernández, "Structural, optical and photocatalytic properties of ZnO nanoparticles modified with Cu," *Materials Science in Semiconductor Processing*, vol. 37 pp. 87-92, 2015.
- [16] T. Dikici, "Temperature-dependent growth of ZnO structures by thermal oxidation of Zn coatings electrodeposited on steel substrates and their photocatalytic activities," *Ceramics International*, vol. 43, no. 11, pp. 8289-8293, 2017.
- [17] F. Wu, C. Wang, H. Marvin, K. Vinodgopal, and G.P. Dai, "Large area synthesis of vertical aligned metal oxide nanosheets by thermal oxidation of stainless steel mesh and foil," *Materials*, vol. 11, no. 6, p. 884, 2018.
- [18] H. Rojas-Chavez, H. Cruz-Martínez, F. Montejo-Alvaro, R. Farías, Y. M. Hernández-Rodríguez, A. Guillen-Cervantes, and O. E. Cigarroa-Mayorga, "The formation of ZnO structures using thermal oxidation: How a previous chemical etching favors either needle-like or cross-linked structures," *Materials Science in Semiconductor Processing*, vol. 108, p. 104888, 2020.
- [19] I. Boukhoubza, M. Khenfouch, M. Achehboune, B.M. Mothudi, I. Zorkani, and A. Jorio, "X-ray diffraction investigations of nanostructured ZnO coated with reduced graphene oxide," *Journal of Physics: Conference Series*, vol. 1292, p. 012011, 2019.
- [20] L. Yuan, C. Wang, R. Cai, Y. Wang, and G. Zhou, "Spontaneous ZnO nanowire formation during oxidation of Cu-Zn alloy," *Journal of Applied Physics*, vol. 114, p. 023512, 2013.
- [21] D. Kim, and J. Y. Leem, "Catalyst-free synthesis of ZnO nanorods by thermal oxidation of Zn films at various temperatures and their characterization," *Journal of Nanoscience and Nanotechnology*, vol. 17, no. 8, pp. 5826-5829, 2017.
- [22] S. H. Kim, A. Umar, and Y. B. Hahn, "Growth and formation mechanism of sea urchin-like ZnO nanostructures on Si," *Korean Journal of Chemical Engineering*, vol. 22, pp. 489-493, 2005.
- [23] M. R. Khanlary, V. Vahedi, and A. Reyhani, "Synthesis and characterization of ZnO nanowires by thermal oxidation of Zn thin films at various temperatures," *Molecules*, vol. 17, no. 5, pp. 5021-5029, 2012.
- [24] D. F. Swinehart, "The Beer-Lambert Law," *Journal of Chemical Education*, vol. 39, no. 7, p. 333, 1962.
- [25] J. Leitner, V. Bartunek, D. Sedmidubský, O. Jankovský, "Thermodynamic properties of nanostructured ZnO," *Applied Materials Today*, vol. 10, pp. 1-11, 2018.
- [26] N. S. Ridhuan, K. A. Razak, Z. Lockman, and A. A. Aziz, "Structural and morphology of ZnO nanorods synthesized using ZnO seeded growth hydrothermal method and its properties as UV sensing," *PLOS ONE*, vol. 7, no. 11, p. e50405, 2012.
- [27] R. Ma, L. Xiang, X. Zhao, and J. Yin, "Progress in Preparation of Sea Urchin-like Micro-/Nanoparticles," *Materials*, vol. 15, pp. 2846, 2022.
- [28] M. Ballesteros-Balbuena, G. Roa-Morales, A. R. Vilchis-Nestor, V. H. Castrejón-Sánchez, E. Vigueras-Santiago, P. Balderas-Hernández, and M. Camacho-López, "Photocatalytic urchin-like and needle-like ZnO nanostructures synthesized by thermal oxidation," *Materials Chemistry and Physics*, vol. 244, p. 122703, 2020.
- [29] Y. A. Shaban, M. A. El Sayed, A. A. El Maradny, R. K. Al Farawati, and M. I. Al Zobidi, "Photocatalytic degradation of phenol in natural seawater using visible light active carbon modified (CM)-n-TiO₂ nanoparticles under UV light and natural sunlight illumination," *Chemosphere*, vol. 91, pp. 307-313, 2013.